25 years anniversary

XMaS the UK Materials Science Beamline

XMaS

NEWSLETTER 2022

CONTENTS

2 | Directors' Corner
3 | Condensed Matter
6 | Materials Science
7 | Soft Matter
8 | Energy & Catalysis
10 | Earth & Environment
11 | Access to Synchrotron and Offline Facilities
12 | Beamline People

ON THE COVER:
Main image, users magnet employed for MXSW (p 5). Clockwise bubbles: Crystalline phase of an organic semiconductor; Bent-rod molecules in columnar liquid crystals (p 7); Partial magnetisation reversal in the top magnetic layer (p 4).

25 years of user operation!

We are extremely proud that XMaS has been supporting users for over 25 years **[1]** *and would like to thank all of the XMaS community for supporting us in developing the facility. XMaS is now fully embedded in the infrastructure for UK large scale light sources* **[2]** *and, we hope, will continue to run for many years to come.*

Although the last few years have been challenging, we are excited that we are now back to full user operations and able to exploit fully the ESRF EBS upgrade. In the last newsletter we highlighted the changes on the beamline in terms of infrastructure and capabilities and we have continued to build on these core developments. The KB mirror assembly is nearing completion and delivery to the facility is expected in the spring of 2023, ready for user experiments from the autumn. This will use the unfocused beam to deliver a tuneable beam size down to a few microns for energies less than about 15 keV. A new 7 element Ge detector for spectroscopy experiments has been ordered to facilitate studies on low concentration samples at high energies (> 25 keV), again this should be delivered in the early summer 2023. At the same time, we are also updating the suite of energy dispersive detectors to include both a single and 4 element 1 mm Si detector for mid-energy spectroscopy as well as diffraction and scattering experiments that require energy discrimination.

In recognition of the need to continue to expand our correlative characterisation capabilities we have ordered a mass spectrometer and gas flow handling system which will be incorporated directly into the beamline control system for operando experiments. A new Potentiostat / Galvanostat will replace the somewhat antiquated current system. In addition, we will be incorporating a Raman system into the beamline to allow Raman spectroscopy simultaneously with the broad range of X-ray techniques that can be undertaken on the beamline. Much of this equipment will also be available for use in the offline laboratory for experiments that do not require the use of X-rays.

As a facility one of our strengths is in developing new sample environments in partnership with users and we welcome collaborations to further expand the capabilities for user driven science. However, we are still being affected by the legacy effects of COVID and Brexit with delays in the delivery of parts which can make modifications for new setups more complex and time consuming. Please get in touch as early as possible if you want to discuss any new sample environment developments.

In staff news, we are pleased to welcome Dr Olga Filimonova to the team. Her expertise in applying spectroscopic techniques to geological materials and minerals broadens further the know-how of the onsite staff. We look forward to introducing the team and the new beamline capabilities to the user community at our User Meeting which will be held in the early summer 2023.

Other changes in the background relate to the chairs of the Project Management Committee (PMC) and the Peer Review Panel (PRP). Chris Nicklin (DLS) is taking over from Peter Hatton (Durham) as chair of the PMC and Rosa Arrigo (Salford) replaces Roger Johnson (UCL) as chair of the PRP. We are indebted to both Peter and Roger for all their help and support over the years.

With the lifting of COVID restrictions it was fantastic that we were able, with the help and support of the ESRF, to re-launch the XMaS Scientist Experience with the 7th edition coming to the beamline during June 2022 **[3]**. The competition to select the winners for the 8th trip was launched in January 2023.

Case studies, especially for the wider audience, are always welcomed and we would like to thank those who helped us to create a schools-based activity sheet and information pack about the science performed on the beamline **[4]**. If any of our users would like to work with us in producing outreach materials, please get in touch as we may be able to provide some support.

Finally, the current XMaS grant funding comes to an end in November 2023, and we are actively working with the community to present a strong case to EPSRC for continued funding. We thank everybody who supported and contributed to the recent "Statement of Need" process and especially thank the staff and users of the Diamond Light Source for their support. We hope to be able to continue to deliver the XMaS facility to you, the user community, for many years to come.

Malcolm Cooper, Yvonne Gründer, Tom Hase and Chris Lucas

[1] http://tinyurl.com/5c7hrxy2
[2] https://tinyurl.com/43s582wd
[3] https://tinyurl.com/4vf3srm3
[4] https://doi.org/10.33424/FUTURUM245

Kondo charge accumulation

C.D. O'Neill, J.L. Schmehr, H.D.J. Keen, L. Pritchard Cairns, D.A. Sokolov, A. Hermann, D. Wermeille, P.I. Manuel, F. Krüger, A.D. Huxley

UAu_2 shows non-Fermi liquid behaviour that is robust in magnetic field **[1]** and is not obviously tied to a quantum critical point. Measurements at XMaS reveal that charge degrees of freedom may play a pivotal role in forming this unusual state.

The third law of thermo-dynamics requires that entropy (or randomness) must vanish for any system *in equilibrium* approaching the absolute zero of temperature. Local moments that are free to point in any direction cannot therefore persist. Magnetic order and Kondo physics provide two escape routes. In the latter the moments are screened by conduction electrons. If spin and charge are inseparable in the electronic screening, the magnetic screening would be accompanied by an accumulation of (negative) charge around the moment site. Charge and spin are however decoupled in a more formal theory, which considers scattering in a single orbital channel, mapping the problem to one dimension (in which spin and charge excitations are separate). In reality, a small change in the local charge density, albeit much weaker than given by the naïve picture of each local moment capturing a single electron, might be expected. Such a change of charge density has however not been detected to date.

For a regular array of Kondo sites, constructive interference could amplify the signal from charge accumulation and be detectable with X-ray diffraction. The problem is that the periodicity of the crystal lattice itself gives a much stronger charge contrast that will hide this signal. To avoid this, Kondo screening incommensurate with the lattice is required, which sounds like an impossible request. UAu_2 however may achieve just this by combining both the escape routes mentioned above. It has an incommensurate magnetically ordered state below a Néel temperature T_N, that our results suggest is accompanied by an incommensurate Kondo state **[1]**.

The observed diffraction intensity from magnetic and charge modulation, measured at XMaS/BM28, are shown in Fig. 1. The magnetic signal was measured with neutrons, but also confirmed with X-rays with a wavelength carefully tuned to an absorption edge (uranium M_4). The charge modulation was measured with much higher X-ray intensity away from the edge and occurs with half the period (twice the wavevector). A small lattice modulation induced by the magnetic order due to magnetostriction can explain some of the charge signal. However, at low temperature the magnetic intensity saturates, but the charge intensity continues to grow. A significant contribution to the charge response is therefore characterised by a lower characteristic temperature scale than the Néel temperature. It could be due to charge accumulation, brought about by Kondo screening with Kondo temperatures lower than T_N.

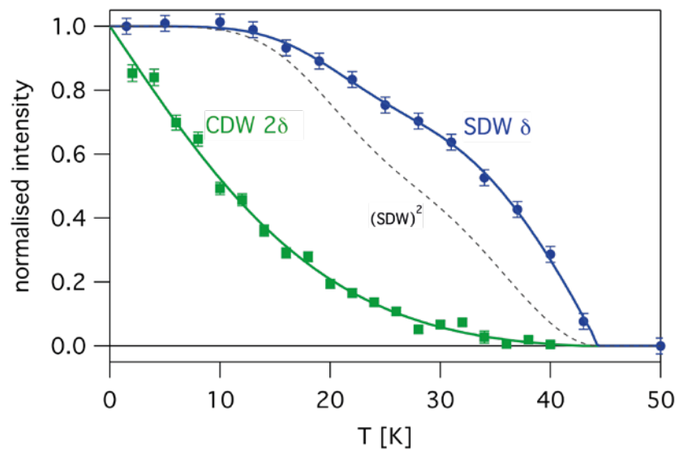

Fig. 1: The upper (blue) line shows the magnetic diffraction intensity. This saturates at low temperature. The lower (green) line shows the charge diffraction intensity, which is at twice the modulation wavevector (half the period). This has a different temperature dependence. The square of the upper curve is also plotted, which would be the form of the charge signal if due to lattice modulation arising from magnetostriction alone.

[1] C.D. O'Neill *et al.*, PNAS 118, 49 (2021).

For more information, contact

A.D. Huxley, School of Physics and Astronomy,
University of Edinburgh, UK.

a.huxley@ed.ac.uk

Near interface magnetisation reversal in spintronic bilayers

D.M. Burn, R. Fan, O. Inyang, M. Tokac, L. Bouchenoire, A.T. Hindmarch, P. Steadman

When electrical current flows through a heavy metal layer adjacent to a ferromagnetic layer, a spin-orbit (SO) torque is exerted on the magnetic spins within the ferromagnet [1]. This link between electronics and magnetic materials is significant for the development of novel technological devices for memory and processing applications in a field known as spintronics.

Our work reveals new insights into the current-driven magnetisation reversal process within a CoFeTaB/Pt bilayer. The strong SO coupling in the Pt heavy metal layer converts the flow of electrical charge into a torque. This torque is exerted on the near interfacial region of the soft ferromagnetic layer and rotates the magnetisation at an angle perpendicular to the current flow direction [2].

X-Ray Reflectivity (XRR) techniques have been used to provide a non-destructive probe to explore both the depth-dependent chemical and magnetic structure within the samples. The chemical contrast is obtained through the difference in the scattering length density (SLD) from the different layers and from the ability to tune the X-ray energy to resonant absorption edges. When probing at one of these absorption edges, differences in the X-ray absorption also occur due to X-ray Magnetic Circular and Linear Dichroism (XMCD and XMLD) which provides insight into the magnetisation orientation within the sample [3]. Our XRR measurements were performed with *in-situ* magnetic fields and electrical currents. Our work combines hard and soft X-ray measurements at XMaS/BM28-ESRF and at I10 - Diamond Light Source, respectively.

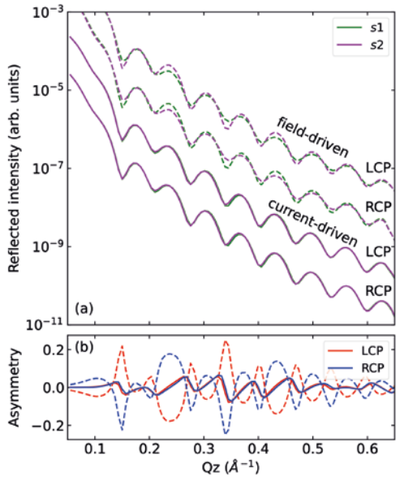

Fig. 2: (a) XRR at the Co L_3 edge with LCP and RCP light after saturating with a magnetic field or electrical current [2] and (b) corresponding asymmetry defined as (s1-s2)/ (s1+s2).

The soft X-ray measurements in Fig. 2a show XRR at the Co L_3 edge where an asymmetry ratio occurs (Fig. 2b) between the saturated states obtained by both magnetic field and current-driven processes. This asymmetry is inverted when changing the handedness of the X-ray polarisation for the field-driven case but not for the current-driven case. Detailed analysis of these results shows how the field reverses the magnetisation of the entire CoFeTaB thickness along the field (and beam propagation) direction, whilst the current reorients a near interfacial region of the CoFeTaB perpendicular to the current flow (and beam propagation) direction [2].

Hard XRR at the Pt L_3 edge is shown in Fig. 3. These results have been fitted and allow the depth profile of the sample to be determined (Fig. 3.c). Furthermore, the asymmetry between measurements with left and right circular polarisation (LCP and RCP) provides information on the depth-dependent magnetisation. A proximity induced magnetisation is found in the Pt at the CoFeTaB/Pt interface [4].

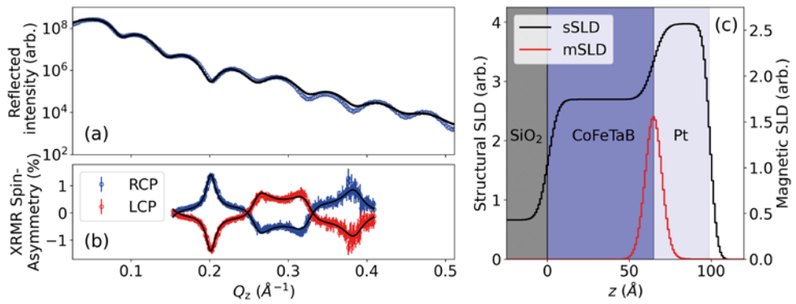

Fig. 3: (a) XRR at the Pt L_3 edge with LCP and RCP light and (b) corresponding asymmetry ratio, which is fitted to extract the structural and magnetic depth profile showed in (c) [2].

These results highlight the power of synchrotron based XRR techniques to explore depth dependent magnetisation behaviour in spintronic multi-layered structures. These techniques allow us to probe the behaviour in the samples with *in-situ* conditions including magnetic fields and electrical currents. Our measurements on CoFeTaB/Pt provide a deeper understanding of the magnetisation reorientation mechanism in layered structures and contributes towards the development of future spintronic device technologies.

[1] T. Nan *et al.*, Phys. Rev. B 91, 214416 (2015).
[2] D.M. Burn *et al.*, Phys. Rev. B 106, 094429 (2022).
[3] G. van der Laan *et al.*, Coor. Chem. Rev. 277, 95 (2014).
[4] O. Inyang *et al.*, Phys. Rev. B 100, 174418 (2019).

For more information, contact
D.M. Burn, Diamond Light Source, UK.
david.burn@diamond.ac.uk

Probing magnetism with X-ray Standing Waves

M. Kamiński, P. Pokhriyal, H. Schulz-Ritter, M. Tolkiehn

The famous phase problem in crystallography can be overcome experimentally using interference of the electromagnetic waves. Multi-beam diffraction and X-ray Standing Waves (XSW) are well-established phase-sensitive methods for direct atomic structure determination. However, no direct X-ray technique based on interference phenomena exists for studying the magnetic structure of crystalline materials. Our work aims at filling this gap by developing a technique based on the standard XSW method.

In the XSW technique, a standing wave formed from the interference between incident and Bragg reflected waves causes modulations in the absorption rate (and also in the fluorescence signal measured experimentally), which are characteristic of the distribution of the given atomic species present in the lattice [1]. An additional sensitivity to the magnetic moments of the atoms is gained by combining XSW with X-ray Magnetic Circular Dichroism (XMCD). The position, element and magnetic sensitivity of the combined techniques thus allows a direct study of the magnetic moments' distribution in a material. The method is foreseen to have indisputable advantages with respect to neutron diffraction, as the magnetic XSW method can be easily applied to thin films.

Fig. 4 presents schematically the idea of the new method using magnetite (Fe_3O_4) as an example. The standing wave has the periodicity of the lattice and moves by half of its period during the rocking scan. When the antinodes of the interference field coincide with a given magnetic sublattice, only this sublattice gives a contribution to the observed magnetic dichroic signal. This effect thus results in a modulation in the XMCD, which gives a direct information about the magnetic ordering.

In a recent experiment, we used an yttrium-iron-garnet ($Y_3Fe_5O_{12}$) single crystal, which exhibits a ferrimagnetic ordering and two magnetic sublattices. This system was chosen to demonstrate the sensitivity of the magnetic XSW to the magnetic ordering. In order to avoid non-magnetic artefacts related to the switching of the incident X-ray beam polarisation, the data were collected with the sample kept in a constant magnetic field, whose orientation was then reversed to evaluate the artefact-free XMCD signal. From the experimental signal we could conclude that in the applied field the magnetic moments of the YIG crystal align along the field lines while antiferromagnetic coupling between the sublattices is suppressed.

One may expect that the same measurement repeated in a weaker magnetic field, which would not suppress the coupling between the sublttices, but only reorient the net magnetic moment, would provide a signal showing the ferrimagnetic nature of YIG.

In the future, assuming that a measurement of the XMCD data without any external magnetic field is feasible, the method could potentially be used to study spontaneous magnetic ordering in ferri/-antiferromagnetic crystals and thin films.

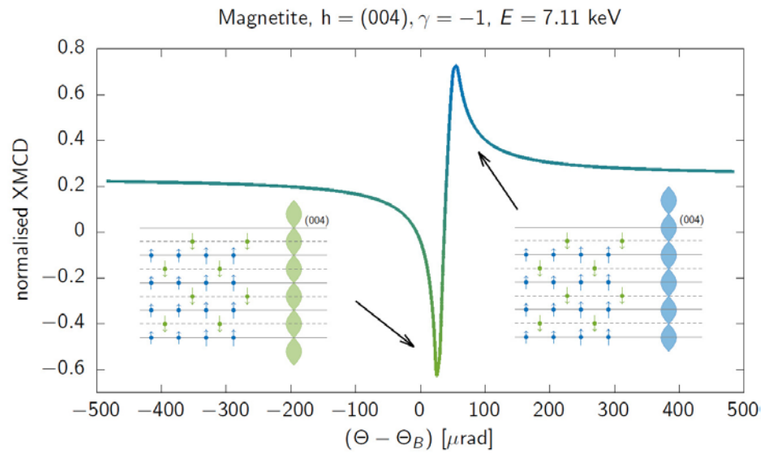

Fig. 4: The idea of the magnetic X-ray Standing Waves method. The standing wave causes a variation in the XMCD, which gives directly information about the magnetic structure of a material.

[1] J. Zegenhagen, Surf. Sci. Rep. 18, 199 (1993)

For more information, contact
M. Kamiński, DESY, Hamburg, Germany (current address: KIT, IPS, Karlsruhe, Germany).
michal.kaminski@kit.edu

TXRF on XMaS: Environmental Quantification

L. Borgese, D. Eichert, T. Hase, D. Wermeille

The environmental impact of noxious materials such as heavy metals is well known. To protect public health, there are statutory limits on the contamination levels for several elements such as lead (Pb) in the environment with specific thresholds in both water and particulate matter (PM) **[1]**.

Several analytical chemical methods are currently used but these can be time consuming and expensive. X-ray Fluorescence (XRF) performed below the critical angle of a reflector is referred to as total reflection XRF (TXRF). It has the advantage of low substrate background and enhanced amplification of the fluorescence emission intensities due to both the incident and reflected beams contributing to the exciting electric field.

We exploited the flexibility of the XMaS diffractometer and detectors to undertake a series of experiments exploring the detection limits, experimental configurations and spatial distribution of analytes in various environmental samples using TXRF. Fig. 5 shows the emission from a ~3 mm droplet of an ICP multi-element standard solution IV (Merck) which was diluted to a concentration of 1 ppb. The results are fully consistent with data obtained from commercial bench-top spectrometers **[2]**. Extrapolating our data show that the limit of detection on XMaS is below the picograms.

Monitoring air quality often involves passing a known volume of air through clean filters and analysing the collected PM. Probing such samples with X-rays removes the need to digest the filter and limits sample handling steps. However, the use of air-filters requires a new approach to sample preparation such as the Smart Store® solution developed by Smart Solution srl and deployed on XMaS during our experiment (Fig. 6). Fig. 5 also shows the emission spectra of $PM_{2.5}$ particles of the multi-element NIST 2783 reference material as well as a single element reference with a Pb mass deposition of 0.59 ± 0.05 μg/cm² **[3]**. Although spectra were easily obtained, these PM samples do not formally comply with the requirements for TXRF quantification. Unfortunately, there are no readily accepted standards nor reference materials to elaborate suitable quantitative procedures. To address this problem, a new ISO standard is currently being developed within the technical committee TC201 (AWI 23971 "Analysis of air PM filters by XRF under grazing incidence").

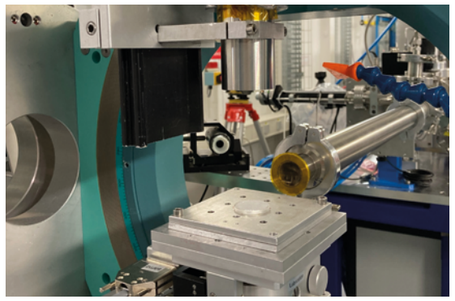

Fig. 6: Experimental setup and $PM_{2.5}$ filter prepared with the Smart Store® solution.

The XMaS/BM28 data were recorded as a function of critical instrumental parameters to provide benchmarking data for the standard, including the impact of the incident angle and beam size. These data are fundamental to the proper development of reference materials and the exploitation of TXRF for environmental studies in the future.

This article is based on work supported by the COST Action ENFORCE TXRF, CA18130 **[4]**.

[1] EC 2018 Clean air policy.
[2] L. Borgese *et al.*, Talanta 181, 165 (2018).
[3] P. Cirelli *et al.*, Spectrochim. Acta Part B 192, 106414 (2022).
[4] enforcetxrf.eu

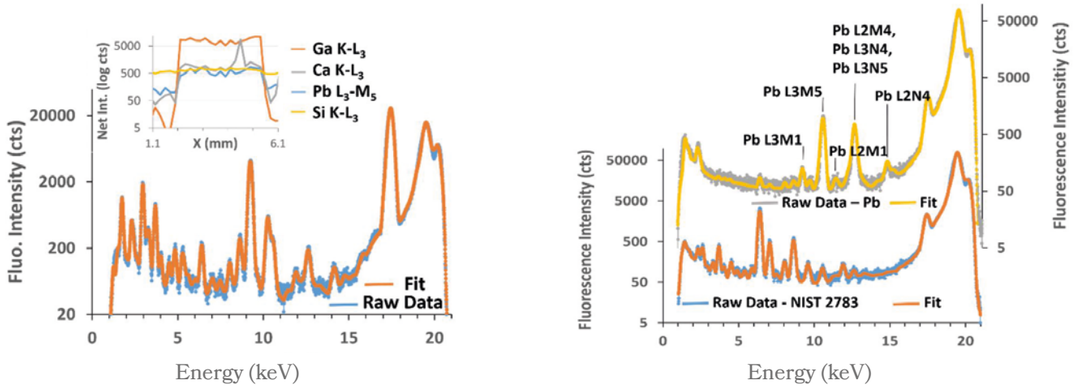

Fig. 5: TXRF spectra of (left) ICP multi-elemental standard solution IV; 5 μl droplet, 1 μg/L on quartz carrier (insert) with selected elemental distributions across the dried droplet residue; (right) TXRF spectra of NIST 2783 reference material and of a single element Pb reference sample. Incident energy: 20.2161 keV; counting time: 300 s (except insert 10 s).

For more information, contact

L. Borgese, Department of Mechanical and Industrial Engineering,
University of Brescia, Italy.

laura.borgese@unibs.it

Spontaneous self-assembly of straight- and bent-rod molecules into a liquid crystal phase of counter-rotating chiral columns

Y.X. Li, H.F. Gao, R.B. Zhang, K. Gabana, Q. Chang, G.A. Gehring, X.H. Cheng, X.B. Zeng, G. Ungar

A much-studied question in biology is why most amino acids in nature are strictly left-handed, causing the alpha-helix in proteins to be right-handed. While in proteins and DNAs the underlying molecular structures are chiral, in achiral compounds spontaneous mirror symmetry breaking can happen, resulting either in right- or left-handed structures. This is an intriguing self-ordering phenomenon and has huge application potentials, e.g. in pharmaceutical industry.

In columnar liquid crystals, overall helical chirality can be induced by inclusion of chiral chemical groups or dopants; these bias molecular twist to either left or right, analogous to a magnetic field aligning the spins in a paramagnet. In a recent work, however, we show that liquid-crystalline columns with long-range helical order can form by spontaneous self-assembly of straight- or bent-rod molecules (Fig. 7a) without inclusion of any chiral moiety. **[1]**

Normal columnar hexagonal phase was observed at higher temperatures for all compounds, without any long range long-range chiral order in the columns formed by the molecules. However, on cooling a complex lattice with *Fddd* symmetry is found. With the help of small and wide angle X-ray diffraction (XRD), and in particular the grazing incidence XRD on oriented thin films (Fig. 7b), we are able to determine the structure of the phase. Reconstructed electron density maps (Fig. 7c,e) reveals that the structure consists of 8 chiral helical columns in the unit cell (4 right-, 4 left-handed). In bent-rod compounds, three molecules back-to-back form a three-arm star, and in straight-rod compounds there are two parallel molecules at each stratum (Fig. 7d,f). In each column the orientation of the molecules changes monotonically with increasing z-elevation, characterises this "antiferrochiral" structure. In selected compounds, it allows close packing of their fluorescent groups reducing their bandgap and giving them promising light-emitting properties.

[1] Y.X. Li *et al.*, Nat. Comm. 13, 384 (2022).

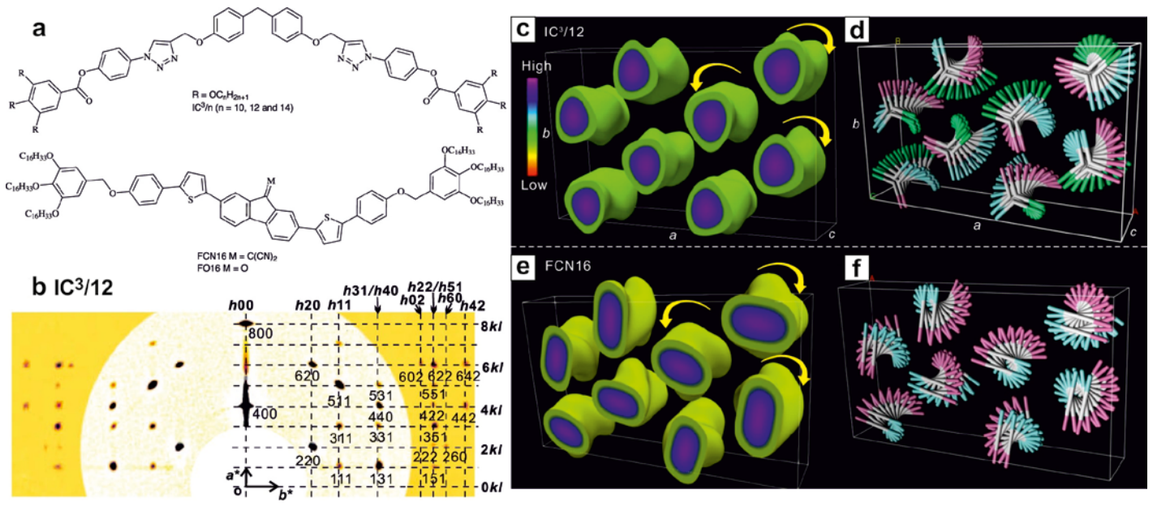

Fig. 7: (a) Chemical formulae of bent- and straight-rod compounds studied.
(b) GISAXS (Grazing Incidence Small Angle X-ray Scattering) diffraction pattern of an oriented thin film in the *Fddd* phase (XMaS/BM28, ESRF).
(c,e) Reconstructed electron density maps of *Fddd* phase formed by bent- and straight-rod compounds, respectively.
(d,f) Schematic models showing how bent- and straight-rod molecules forming co- and counter-rotating helical columns leading to the complex *Fddd* symmetry.

For more information, contact

X. Zeng, Department of Materials Science and Engineering,
University of Sheffield, UK.

x.zeng@shef.ac.uk

Surface resonant X-ray diffraction probing the charge distribution at an electrochemical interface

Y. Gründer, C.A. Lucas, P.B.J. Thompson, Y. Joly, Y. Soldo-Olivier

Electrochemistry underpins many current technologies and plays a crucial role in the development of new energy storage applications. Electrochemistry deals with reactions that involve transfer of electrical charges at interfaces between an electrode and chemical species in solution. Although there have been several theoretical studies of the charge transfer mechanism, few experimental electrochemical investigations are reported, due to the complexity of the electrochemical environment which makes the interface inaccessible to traditional electron-based probes of charge transfer. A fundamental understanding of the nature of the charge transfer and the electron distribution at the interface is therefore a major goal in electrochemistry.

We have employed Surface Resonant X-ray Diffraction (SRXRD) in combination with self-consistent DFT calculations to assess the charge distribution and bonding mechanism for the adsorption of bromide anions onto a single crystal Cu(001) electrode surface **[1]**. The X-ray scattering amplitude depends on the electron density of the contributing atoms: any modification of charge distribution should be observable in a change of the scattered intensity close to the adsorption edge of the involved atoms. The intensity variation at each position in reciprocal space is thus specific to the spectroscopic response of the probed atoms and to the modification of their atomic form factor due to the change in the electron arrangement at the interface (Fig. 8).

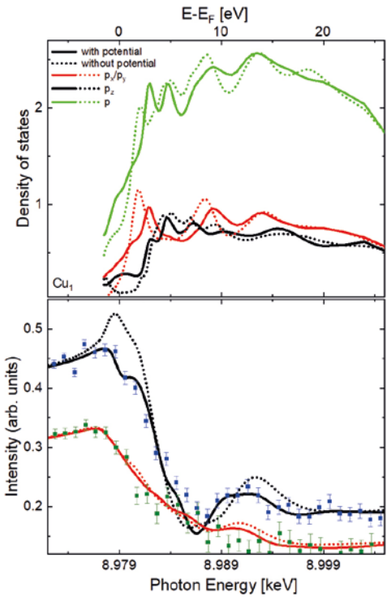

Fig.8: The spectra at the surface sensitive anti-Bragg position (1 1 0.2) measured in horizontal and vertical polarisation modes are shown (lower panel) together with the modelled data obtained both with (full line) and without (dotted line) the additional Helmholtz potential. The changes in the empty states of the electron density of the 4p-orbitals of the first atomic layer are shown to illustrate the changes induced in the spectra.

The electrochemical environment was mimicked by a simple double layer model at the electrochemical interface (Helmholtz description), which has been implemented into the FDMNES code introducing an additional potential **[2]**. Its effect on the electron distribution at the interface (Fig. 9) can be obtained. The charge distribution at the atoms has been altered, not only by adding or subtracting charges, resulting simply in a charged atom, but by a rearrangement of the electron densities.

In addition, the dipole surface moment shifts into the metal electrode. A similar effect with an electric dipole in the metal surface was found with the same method on Pt (111) **[3]**.

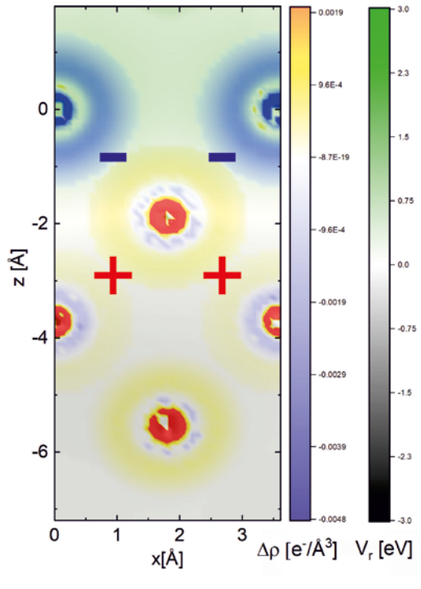

Fig. 9: Map of the difference in electron density Δρ and in the potential energy V$_r$ induced by the Helmholtz potential. It is shown along the [100] direction (bulk coordinates) through the Br adsorbate. The '+' and '-' indicate the additional charge rearrangement from the hybridisation of the orbitals.

These results show that *in-situ* SRXRD studies combined with self-consistent DFT calculations can suitably assess the charge distribution and bonding mechanism of specific adsorbate at the electrochemical interface.

[1] Y. Grunder *et al.*, J. Phys. Chem. C 126, 4612 (2022).
[2] Y. Joly *et al.*, J. Chem. Theory and Computation 14, 973 (2022).
[3] Y. Soldo *et al.*, ACS Catalysis 12, 2375 (2022).

For more information, contact

Y. Gründer, Department of Physics, University of Liverpool, UK.

grunder@liverpool.ac.uk

Understanding interactions between metals and ionic liquids

C. Borrill, S. Booth, A. Nedoma, I. Efimov, S. Qu, K. Lovelock, K. Sedransk Campbell

Ionic Liquids (ILs) offer more environmentally friendly alternative to typical organic chemicals due to properties including low volatility and toxicity, as well as opportunities for solvent recycling **[1]**. These solvents are characterised as salts with a melting temperature of <100°C. They are typically composed of an organic cation, frequently imidazolium or amine-based with a smaller classically inorganic anion. The proximity and/or organisation of the ILs constituents in aqueous solutions has proven intriguing due to the different behaviours observed depending on IL concentration.

Aqueous-IL systems have been reported to offer potential new synthesis routes for metal oxides and waste treatment, however little fundamental understanding exists regarding the underpinning chemistry between metals and ILs. As such, it is critical to establish the bonding chemistries between metals and ILs, considering a breadth of different solution concentrations and conditions. Moreover, this knowledge will improve the assessment of corrosion hazards using these solvents **[2]**.

A widely researched IL, 1-methy-3-butylimidazolium chloride ([Bmim]Cl), has been studied on XMaS/BM28 using X-ray Absorption Near Edge Spectroscopy (XANES). An illustrative example presented here is a case where the solution was doped with $CuCl_2$. Both the Cl and Cu K-edges (2.822 and 8.979 keV, respectively) were investigated.

The Cu K-edge XANES (Fig. 10) demonstrated a clear shift in dominant speciation behaviours observed around the Cu. At low IL concentrations, *e.g.* 98 mol% water in IL, the behaviour is similar to Cu in pure water suggesting that the role of the IL, when found in low concentrations, has little influence, let alone immediate relationship, with the Cu in solution. **[3]**. However, with increasing IL concentration the preferential coordination shifts towards $CuCl_2\ 2H_2O$ **[4]**.

The Cl K-edge spectra (Fig. 11) demonstrate two different categories of behaviours. For low concentrations of IL, *i.e.* above 98 mol% water in IL, a broad peak is unmistakable. However, with increasing IL concentration, *i.e.* 85 mol% water in IL, a prominent major peak with a small secondary shoulder and pre-peak are observed. This is consistent with the pure IL; in this scenario the Cl- preferentially binds with water, rather than the IL **[5]**. Contextualising these results with corresponding Tafel plots obtained in the laboratory, it is evident that these noted distinctions are directly linked to the corrosion mechanisms observed. Tafel polarisation experiments allow corrosion mechanisms to be quickly proved *via* electrochemical experiments. 75 and 85 mol% [Bmim]Cl solutions demonstrate the same result, representative of active corrosion, whereas both 98 and 99 mol% solutions have evidence of passivation reactions.

The experiments undertaken at BM28 have allowed an insight into the complex nature of IL-metal interactions and demonstrated the promise of techniques such as XANES in materials selection for large scale IL implementation.

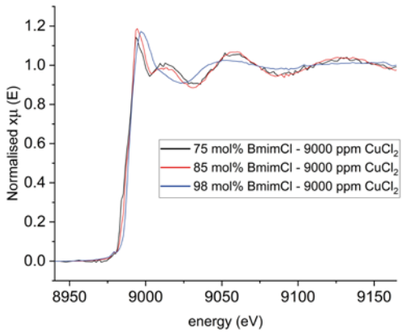

Fig. 10: Cu K-edge XANES of doped [Bmim]Cl solutions.

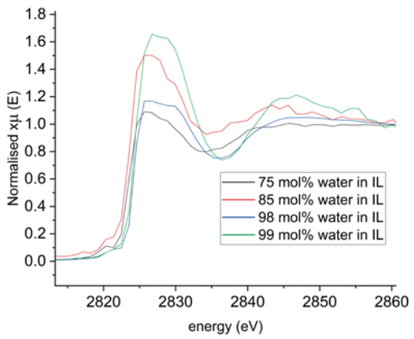

Fig. 11: Cl K-edge XANES for 75, 85, 98, 99 mol% doped solutions.

[1] T. Welton *et al.*, Chem. Rev. 99, 2071 (1999).
[2] I. Perissi *et al.,* Corros Sci 48, 2349 (2006).
[3] A.R. Abouelela *et al.*, ACS Sustain Chem Eng 9, 10524 (2021).
[4] G. la Penna *et al.*, J. Chem. Phys. 143 (2015).
[5] M. Ferrandon *et al.*, J. Therm. Anal. Calorim. 119, 975 (2015).
[6] J.L. Fulton *et al.*, J. Chem. Phys. 125 (2006).

For more information, contact

K.S. Campbell, Department of Chemical and Biological Engineering, University of Sheffield, UK.

k.sedransk@sheffield.ac.uk

X-ray absorption spectroscopy study of the state of Pd in pyritedistribution at an electrochemical interface

O. Filimonova, P. Thompson, D. Wermeille

Pyrite [FeS_2] is an ubiquitous minor sulphide in Cu-Ni-PGE (platinum group elements) magmatic and late magmatic deposits. According to the laser ablation inductively coupled plasma mass spectrometry studies, the content of Pd in natural pyrites varies from few ppb to few tens of ppm (e.g. 60 ppm **[1]**) or even few hundreds of ppm (e.g. 470 ppm **[2]**). The experimental investigation of Pd-Fe-S systems demonstrated that the content of Pd in pyrite can reach a few weight percent **[3]**. The state of Pd in pyrite, including oxidation state and local atomic environment, however, is still debatable.

In this study, Pd-doped pyrite crystals were synthesized using a salt flux technique at a steady-state temperature gradient at 650/580 °C at the hot/cold end of the ampoule **[4, 5]**. Crystals containing 1.9 wt.% of Pd were mounted in epoxy resin and polished. The sample was then studied using X-ray absorption spectroscopy at XMaS/BM28 in fluorescence mode at the Pd K-edge (24350 eV). Comparison of the XANES spectra of the sample and Pd-bearing standards showed that the formal oxidation state of Pd in pyrite is close to +4 (blue insert in Fig. 12). The results of FDMNES simulation **[6]** are shown in Fig. 12. The best simulation of the experimental spectrum is achieved when Pd substitutes for Fe in the cationic site of pyrite. The EXAFS spectrum fit confirmed that Pd forms a solid solution in pyrite substituting Fe in the cationic subshell (Fig. 13).

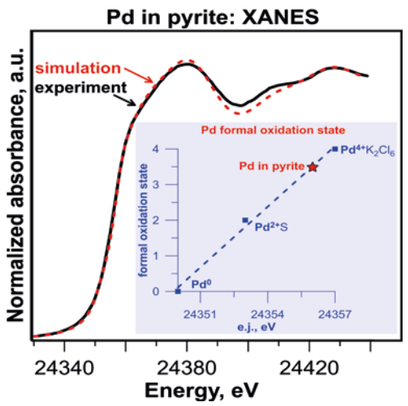

Fig.12: Normalised Pd K-edge XANES of Pd-bearing pyrite together with FDMNES simulation (Pd in the solid solution: 4 × 4 × 4 supercell structure, 5 Å cluster radius). (insert) Formal oxidation state in standards and sample as a function of the position of e.j. (eV). The dashed line corresponds to the linear regression through the experimental data points. The red star indicates the sample. Formal oxidation state of Pd in pyrite is close to +4.

The interatomic distance Pd-S of 2.39 ± 0.01 Å is much longer than that of Fe-S in pure pyrite (RFe-S = 2.26 Å **[7]**). The expansion caused by the incorporation of Pd in the FeS_2 structure disappears in the second coordination shell where interatomic distances are close to the typical distances of the Fe local atomic environment in FeS_2. We note that the ionic radii of Fe^{2+} (0.61 Å) and Pd^{4+} (0.62 Å) are close thereby favouring the formation of the solid solution.

Our solubility data combined with the other experimental studies of the concentration of Pd in pyrite **[3, 9]** showed that the Pd content increases sharply with the increase of the temperature. The calculated Pd content in pyrite at 300 °C can be estimated as < 1 ppb, 400 °C – 2 ppm, 500 °C – few hundreds of ppm and at 600 °C – few weight per cents.

The results of our experiment, combined with the data on the concentration of Pd in pyrite allow: (i) the physico-chemical modelling of Pd migration and precipitation in natural systems, (ii) the building or a model capable of describing the concentration of Pd in pyrite, (iii) the development of ores refinement, leaching and extraction technologies.

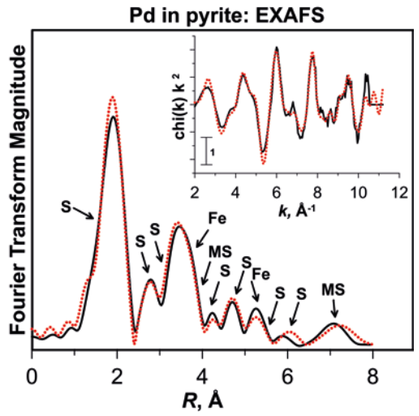

Fig. 13: Fourier Transforms of the k^2-weighted background-subtracted EXAFS spectra (not corrected for phase shift) (black line) and fit obtained with the ARTEMIS program [8] (red dotted line) at the Pd K-edge. (insert) k^2-weighted EXAFS spectrum. The contributions from different coordination shell are shown with arrows.

[1] R. Piña *et al.*, Miner Deposita, 51 (7), 853 (2016).
[2] L.J-P. Cabri *et al.*, 9th International Congress for Applied Mineralogy ICAM, 9 (2008).
[3] E. Makovicky, S. Karup-Møller, Mineral. Mag. 59 (397), 685 (1995).
[4] D.A. Chareev, Cryst. Rep., 61 (3), 506 (2016).
[5] D.A. Chareev *et al.*, Crystallogr. Rep. 61(4), 682 (2016).
[6] Y. Joly, Phys. Rev. B 63, 125120 (2001).
[7] G. Brostigen. A. Kjekshus, Acta Chem. Scand. 23 (6), 2186 (1969).
[8] B. Ravel, M. Newville, J. Synchrotron Radiat. 12, 537 (2005).
[9] S. Lipko *et al.*, Minerals 15, 12 (9), 1165 (2022).

For more information, contact
O. Filimonova, XMaS and Department of Physics, University of Liverpool, UK.
olga.filimonova@esrf.fr

APPLICATIONS FOR SYNCHROTRON BEAM TIME

Two proposal review rounds are held each year. **Deadlines for applications to make use of the National Research Facility (CRG) time are normally 1st April and 1st October** for the scheduling periods August to February and March to July, respectively.

Applications for beamtime must be submitted electronically via the ESRF web page: www.esrf.eu. Select **"Users & Science"**, then choose **"Applying for beamtime"** from the drop-down list. On the right hand side, you can consult the instructions to submit your proposal and access the **"User Portal"**. Enter your surname and password and select **"Proposals/Experiments"**. Follow the instructions carefully — you must choose **"CRG Proposal"** and **"BM28 (XMaS - Mat.Sci.)"** at the appropriate stage in the process. If you experience any problems, please contact Laurence Bouchenoire (bouchenoire@esrf.fr). Technical specifications and instrumentation available are described on the XMaS web page (www.xmas.ac.uk). All sections of the form must be filled in. Particular attention should be given to the safety aspects with the name and characteristics of your samples completed carefully. Experiments requiring special safety precautions such as the use of electric fields, lasers, high pressure cells, dangerous substances, toxic substances and radioactive materials, must be stated clearly in the proposal. Moreover, any ancillary equipment supplied by the user must conform to the appropriate French regulations. Further information may be obtained from Martine Moroni, the ESRF Experimental Safety Officer for CRG beamlines (martine.moroni@esrf.fr, tel: +33 4 76 88 23 69). Please indicate your date preferences, including any dates that you would be unable to attend if invited for an experiment. This will help us to produce a schedule that is satisfactory for all.
When preparing your application, please consider that access to the National Research Facility is reserved for UK based researchers. Collaborations with EU and international colleagues are encouraged, but the proposal must be led by a UK based principal investigator. It must be made clear how any collaborative research supports the wider UK science base. Applications without a robust link to the UK will be rejected and should instead be submitted directly to the ESRF using their public access route.
Access to the XMaS beamline is also available for one third of its operational time to the ESRF's user community. Applications for beamtime within that quota should be made in the **ESRF's proposal rounds (application deadlines 1st March and 12th September)**. Applications for the same experiment may be made to both XMaS directly and to the ESRF. Obviously, proposals successfully awarded beamtime by the ESRF will not then be given additional time in the XMaS allocation.
An experimental report on completed experiments must be submitted electronically, following the ESRF model. The procedure for submitting experimental reports follows that for the submission of proposals. Please follow the instructions on the ESRF's web pages carefully. **Reports must be submitted within 6 months of the experiment.** Note that the abstract of a publication can also serve as the experimental report! Please also remember to fill in the XMaS end of run survey form on completion of your experiment, which is available on the website (https://bit.ly/3JM6E7q).

Assessment of Applications
The independent Peer Review Panel considers the proposals, grades them according to scientific excellence, adjusts the requested beam time if required, and recommends proposals to be allocated beam time on the beamline. Experimental reports will also form part of the assessment criterion. Proposals which are allocated beamtime must meet ESRF safety and XMaS technical feasibility requirements. Following each meeting of the Peer Review Panel, proposers will be informed of the decisions taken and feedback provided.

APPLICATIONS FOR OFFLINE FACILITY TIME

Submit your application directly on the XMaS web site: www.xmas.ac.uk. Select **"XMaS Offline Facilities"** and then **"Application for Offline Facilities"**. Follow the instructions carefully and do not forget to upload your 1-2 page proposal at the end of the application form. Please contact the local staff to discuss any potential experiments. Successful offline proposals will be run as in-house experiments. We will complete the safety form with the information supplied in your application form as well as arrange site passes and any accommodation that may be required. As for synchrotron beamtime, offline users normally stay in the ESRF guest house or off-site hotels.

The XMaS facility implements transparent policies and procedures to guarantee that access is based on scientific excellence only. In partnership with the ESRF Safety office, we will endeavor to ensure that the facility can accommodate any user, but this may require an individual needs assessment. If you have any questions about accessing the facility at any stage of the application or experimental processes, please do not hesitate to get in touch.

Living allowances
These are €75 per day per beamline user — the equivalent actually reimbursed in sterling. XMaS will support up to 3 users per synchrotron experiment and only 1 on the offline laboratories. For experiments which are user intensive, additional support may be available. The ESRF hostel still appears adequate to accommodate all our users, though CRG users will always have a lower priority than the ESRF's own users. Do remember to complete the "A-form" when requested to by the ESRF, as this is used for hostel bookings, site passes and to inform the safety group of attendees.

Beamline people

ONSITE TEAM

Didier Wermeille
didier.wermeille@esrf.fr
is the Beamline Responsible who, in partnership with the Directors, oversees the activities of the user communities as well as the programmes and developments that are performed on the beamline. He is also the beamline Safety Representative. His expertise spans crystallography, high resolution diffraction, surface studies, magnetic scattering and electric field measurements.

Laurence Bouchenoire
bouchenoire@esrf.fr is the Beamline Coordinator. She looks after beamline operations and can provide you with information about the beamline, application procedures, scheduling, etc. Laurence should normally be your first point of contact. Her expertise is in magnetic scattering including polarisation dependence.

Oier Bikondoa
oier.bikondoa@esrf.fr
is Beamline Scientist with expertise in soft matter materials, (GI-)SAXS/WAXS surface and reflectivity studies.

Edgar Gutierrez Fernandez
edgar.gutierrez-fernandez@esrf.fr
and **Olga Filimonova**
olga.filimonova@esrf.fr are our PDRAs with expertise in scattering and spectroscopy techniques, respectively.

Paul Thompson
pthompso@esrf.fr is the contact for instrument development, technical support, sample environments including electric field, liquid cells and catalysis. He is assisted by **John Kervin** jkervin@liv.ac.uk, who is based at the University of Liverpool but provides further technical back-up and spends part of his time on-site at XMaS.

PROJECT DIRECTORS

Chris Lucas clucas@liv.ac.uk and **Tom Hase** t.p.a.hase@warwick.ac.uk continue to travel between the UK and France to oversee the operation of the beamline.

Malcolm Cooper
m.j.cooper@warwick.ac.uk
remains involved in the beamline operation as an Emeritus Professor at the University of Warwick.

Yvonne Gründer
yvonne.grunder@liverpool.ac.uk
is part of the management team at Liverpool to provide additional support. She also oversees impact activities.

Sarah Jarratt
sarah.jarratt@warwick.ac.uk
and **Julie Clark**
Julie.Clark@liverpool.ac.uk
are the administrators on the project, based in the Department of Physics at Warwick and Liverpool, respectively. Sarah is the point of contact for user T&S claims and co-ordinates the annual XMaS Scientist Experience.

THE PROJECT MANAGEMENT COMMITTEE

The current membership of the committee is as follows:
C. Nicklin (chair), DLS
K. Yeung, EPSRC
M. Alfredsson, Uni. of Kent
M. Cain, Electrosciences Ltd
A. Beale, Uni. College London
K. Edler, Uni. of Bath
B. Hickey, Uni. of Leeds
S. Langridge, ISIS
W. Stirling, Institut Laue Langevin

In addition to the above, the directors, the chair of the Peer Review Panel, the CRG Liaison M. Hahn and the beamline team are in attendance at the meetings which happen twice a year.

THE PEER REVIEW PANEL

The current membership of the panel is as follows:
R. Arrigo (chair), Uni. of Salford
A. Hector, Uni. of Southampton
E. Heeley, Open University
M. Skoda, ISIS
K. Syres, Uni. of Central Lancashire
L. Ishibe-Veiga, DLS

In addition, either Chris Lucas or Tom Hase attends their meetings in an advisory role.

PUBLISH PLEASE!!... and keep us informed

One of the important XMaS KPIs is the number and quality of publications. We ask you to provide Sarah Jarratt (sarah.jarratt@warwick.ac.uk) with the reference and DOI whenever a new paper is published. Alternatively, you can submit your new publication reference directly through a form on our web site (https://bit.ly/2Gja4zX). Please also let us know about other impact generated as a result of XMaS work.

IMPORTANT!
It is important that we acknowledge the support from EPSRC in any publications. When beamline staff have made a significant contribution to your scientific investigation you may naturally want to include them as authors. Otherwise we ask that you add an acknowledgement of the form:

"XMaS is a UK national research facility supported by EPSRC. We are grateful to all the beamline staff for their support."

Editor: Laurence Bouchenoire - Graphic Designer: Sylvie Quercia - Print: Warwick Print - February 2023

XMaS, the UK Materials Science Beamline

ESRF - The European Synchrotron
71 avenue des Martyrs, CS 40220
38043 Grenoble Cedex 9,
France

Tel: +33 (0)4.76.88.25.80
xmas@esrf.fr

@XMaSBeam

www.xmas.ac.uk

XMaS the UK-CRG

UNIVERSITY OF LIVERPOOL

UKRI Engineering and Physical Sciences Research Council

WARWICK THE UNIVERSITY OF WARWICK